Received: 8 October 2020 | Revised: 23 February 2021 | Accepted: 15 March 2021

DOI: 10.1002/hyp.14143

RESEARCH ARTICLE

WILEY

Use of point scale models to improve conceptual understanding in complex aquifers: An example from a sandstone aquifer in the Eden valley, Cumbria, UK

Antoine E. A. Lafare[1,2] | Denis W. Peach[1,3] | Andrew G. Hughes[1]

[1]British Geological Survey, Keyworth, Nottinghamshire, UK

[2]PARATONIC, Jonquières, Languedoc-Roussillon, France

[3]Faculty of Engineering, Department of Civil and Environmental Engineering, Imperial College, London, UK

Correspondence
Andrew G. Hughes, British Geological Survey, Keyworth, Nottinghamshire NG12 5GG, UK.
Email: aghug@bgs.ac.uk

Funding information
NERC Changing Water Cycle programme, Grant/Award Number: NE/I006591/1

Abstract

Understanding catchment functioning is increasingly important to enable water resources to be quantified and used sustainably, flood risk to be minimized, as well as to protect the system from degradation by pollution. Developing conceptual understanding of groundwater systems and their encapsulation in models is an important part of this understanding, but they are resource intensive to create and calibrate. The relative lack of data or the particular complexity of a groundwater system can prevent the development of a satisfactory conceptual understanding of the hydrological behaviour, which can be used to construct an adequate distributed model. A time series of daily groundwater levels from the Permo-Triassic sandstones situated in the River Eden Valley, Cumbria, UK have been analysed. These hydrographs show a range of behaviours and therefore have previously been studied using statistical and time series analysis techniques. This paper describes the application of AquiMOD, impulse response function (IRF) and combined AquiMOD-IRF methods to characterize the daily groundwater hydrographs. The best approach for each characteristic type of response has been determined and related to the geological and hydrogeological framework found at each borehole location. It is clear that AquiMOD, IRF and a combination of AquiMOD with IRF can be deployed to reproduce hydrograph responses in a range of hydrogeological settings. Importantly the choice of different techniques demonstrates the influence of differing processes and hydrogeological settings. Further they can distinguish the influences of differing hydrogeological environments and the impacts these have on the groundwater flow processes. They can be used, as shown in this paper, in a staged approach to help develop reliable and comprehensive conceptual models of groundwater flow. This can then be used as a solid basis for the development of distributed models, particularly as the latter are resource expensive to build and to calibrate effectively. This approach of using simple models and techniques first identifies specific aspects of catchment functioning, for example influence of the river, that can be later tested in a distributed model.

KEYWORDS
Cumbria, conceptualization, Eden, groundwater, model

1 | INTRODUCTION

Understanding catchment functioning is increasingly important to enable water resources to be quantified and used sustainably, for example Hutchins et al. (2018), flood risk to be minimized, for example Rogger et al. (2017), as well as to protect the system from degradation by pollution, for example Wang and Burke (2017). However, catchments often have a high degree of heterogeneity and complexity in their geology and topography, for example Di Lazzaro et al. (2015), which affects their surface and groundwater hydrology, for example Oudin et al. (2010). To manage such catchments well a good understanding of their functioning is required. This can be achieved with a variety of data analysis approaches. Typically these involve a series of activities: a combination of data gathering and monitoring, the interpretation of these data to develop a conceptual understanding of surface and groundwater flow regimes and the subsequent testing of that understanding using mathematical modelling, for example Abesser et al. (2017). The refinement of the conceptual model and its encapsulation in the numerical model is, by its nature iterative and benefits from the use of different data types to develop understanding and to compare model outputs (Schilling et al., 2019). This sequence of activities or workflow leads, ideally, to the creation of a model with the ability to be used to make forecasts or predictions of future behaviour under differing conditions.

However, these activities are time consuming and require significant resources (i.e. person years of effort), they require access to suitable datasets as well having the appropriate techniques that can be used to successfully analyse these data. The interpretation of time series of observed data from catchments, such as groundwater levels or stream flows, are essential for the understanding the response of catchment hydrological system to the inputs of rainfall and groundwater recharge. To be reliable this analysis and interpretation should be carried out in a systematic and reproducible way and could take the form of statistical analysis, transfer function approaches such as impulse response function (IRF) or relatively simple lumped parameter models. Application of these techniques means that the data can be interrogated efficiently and the conceptual understanding developed and subsequently tested without the need to develop a fully distributed numerical model.

Observed hydrological catchment variables are usually measured sequentially in time, and when collected over a predominantly fixed sampling interval they form a historical time series (Cowpertwait & Metcalfe, 2009), allowing the investigation of temporal behaviour. From a statistical point of view such historical time series can be treated as different sequences of random variables that can be interpreted by time series analysis. Groundwater systems can be conceptualized as filters transforming an input signal (e.g. rainfall) into an output signal (e.g. flow or groundwater level) by application of a transfer function (Delbart et al., 2016; Mangin, 1984). Once defined, these mathematical relationships can be used to help determine the functioning and structure of aquifers. There are number of time series techniques that have been routinely used to characterize groundwater systems, with a range of functions (extensively described by Box et al., 2015) that can offer a systemic and quantified approach to analysing these systems.

An IRF is a way of converting a series of input time series into an output variable. Typically, this consists of a relationship between response factor and time (see Figure 1 for an example) that can take various shapes according to the behaviour of the modelled system. Applied successfully an IRF can define the temporal relationship of the particular input variable, for example rainfall, and the output variable, such as groundwater head. It can help characterize the system response and be related to the physical processes operating in the catchment. Recently, the IRF methodology has been used to analyse groundwater flooding in the United Kingdom to offer explanations for differing observation borehole groundwater level responses to a flooding event in winter 2013/2014 (Ascott et al., 2017). IRFs have also been used to understand the impact of rainfall/drought events and changing groundwater abstraction on groundwater levels in the United States (Russo & Lall, 2017) and to estimate recharge rates to Australian aquifers (Hocking & Kelly, 2016). IRFs have underpinned the development of the Transfer Function Noise approach (von Asmuth et al., 2002) and have been used in understanding time series length required for model calibration (van der Spek & Bakker, 2017).

Deterministic models provide a well-established way of simulating groundwater systems and addressing particular questions such as data gaps, for example in the Dumfries Basin; (Jackson et al., 2005) and the impacts of climate change on water resources, for example in the Berkshire Downs (Jackson et al., 2011). However, a fully distributed, time variant model can often be resource-intensive to develop and relies on a mature understanding of groundwater flow in the aquifer and a well-developed conceptual model for its ability to reproduce observed behaviour. Where resources, data or understanding are less available lumped parameter or point models offer a parsimonious method by which the conceptual understanding of the observed groundwater level response at a borehole can be tested. These are relatively simple models, which represent parts of the hydrological system as a series of interconnected single stores which can represent different volumes in the system. They are often applied in situations

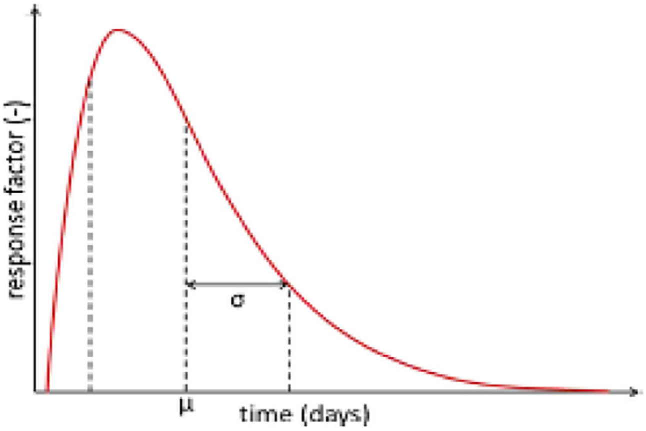

FIGURE 1 Example of impulse response function (IRF) response curve (μ – mean; σ – 1 standard deviation)

where there is insufficient data to adequately parameterise a distributed model or where the hydrogeology appears so complicated or uncertain that this is the only way that it can reasonably be mathematically represented. Recent examples of the application of lumped parameter models are found in Mackay et al. (2014a, 2014b) who demonstrate the application of different model structures using the AquiMOD code (Mackay et al., 2014a, 2014b) to help improve conceptual understanding and simulate groundwater hydrograph responses in a range of different UK aquifers. Lumped models have been used to simulate discharge to rivers from aquifers (Anaya & Wanakule, 1993; Rozos et al., 2004), and water levels in a representative observation well within the aquifer (Barrett & Charbeneau, 1997; Scanlon et al., 2003) or head gradient towards a river (Hughes, 2004).

To explore how simpler approaches, which stop short of a fully distributed model, can be applied to develop conceptual understanding a case study in the Permo-Triassic sandstone in the Eden Valley, Cumbria has been used. A systematic study of the available groundwater level time series data was, therefore, undertaken by the application of AquiMOD, IRF and combined AquiMOD-IRF methods to daily hydrographs. The geological and hydrogeological framework of the study area, the groundwater level data set and AquiMOD and the IRF methods (basic and stress related implemented in AquiMOD) are outlined. The AquiMOD model code applied to study the variation between the different borehole groundwater responses is described and the subsequently obtained results presented. Following on from this, the IRF methods, both basic and stress-related, are presented and described. Finally, the implications for understanding the recharge and groundwater flow processes operating in the Eden Valley Permo-Triassic sandstone aquifers are discussed, with reference to the results from the application of both AquiMOD, IRF and the combined AquiMOD-IRF approach to analyse the groundwater level time series.

2 | METHODOLOGY

2.1 | Study area

The River Eden Valley (Cumbria, UK) is a large rural area with a relatively low population density, in which agriculture and tourism provide the main sources of income. Permo-Triassic sandstones form the major aquifers in the region and have the potential to provide significant groundwater resources (Butcher et al., 2006). A number of water management issues have been identified, which operate over a wide range of scales for this area, including flooding (Leedal et al., 2013; Mayes et al., 2006), pollutant transport, particularly nitrates (Wang & Burke, 2017) and ecology (Hulme et al., 2012). However, there is no detailed conceptual model and associated numerical groundwater model for the Permo-Triassic sandstone aquifers in the Eden Valley, which could be used to address these issues. Moreover, any investigation of the impact of climate change on the groundwater flow in the River Eden catchment would require a reliable understanding of the aquifers' responses to recharge at different time scales.

2.2 | Geological and hydrogeological setting

The Permo-Triassic rocks of the Eden Valley lie in a fault-bounded basin (Stone et al., 2010) (approximately 50 km long and 5–15 km wide) that is straddled to the southwest by the high ground of Lake District and to the northeast by the hills of the North Pennines (Figure 2). This basin contains Permian and Triassic strata (see Table 1) which dip gently to the north east (Figure 2). The Pennine Fault and associated North Pennine escarpment form the eastern boundary of what has been interpreted as a half-graben, resulting in Permo-Triassic rocks outcropping against Carboniferous or Lower Palaeozoic rocks. To the west, the Permo-Triassic succession wedges out against the underlying Carboniferous strata (Allen et al., 1997), which consist of a sequence of layers of limestones, sandstones, mudstones and coals (Table 1; Figure 2).

The Penrith Sandstone formation, which lies unconformably over the Carboniferous, was deposited in a structurally-controlled intermontane basin orientated along the present Eden Valley. These sandstones, mostly of aeolian origin, reach a thickness of about 900 m in the centre of the basin (see cross-section; Figure 3). The basal breccias locally known as Brockram become progressively more dominant southwards. This is composed of angular fragments of dolomitised limestone embedded in a strongly cemented calcareous sandstone matrix (Millward, 2004). The Penrith sandstone (Hughes, 2003) itself consists of well-rounded and well-sorted, medium to coarse grains. Less well-sorted finer grained sandstone beds with thin mudstone intercalations are common, mainly at the top of the sequence and at the margins of the basin, indicating episodes of fluvial deposition. In the northern part of the basin, parts of the top 100 m of the formation have been secondarily cemented by silica. Where such cement is abundant, the relief is stronger (Hughes, 2003; Millward, 2004; Stone et al., 2010). These cemented sandstones are much indurated and exhibit a very low hydraulic conductivity (Butcher et al., 2006; Waugh, 1970), lower down in the sequence the Penrith sandstones are moderately cemented and form some of the most permeable strata of the Permo-Triassic sandstones of the Eden Valley (Allen et al., 1997).

The Eden Shale Formation overlies the Penrith Sandstone (Figure 3) and is formed of mudstone and siltstone; sandstone, breccias and conglomerate intercalations being subordinate. Gypsum and anhydrite (at depth) are present as beds, nodules, cements and veins (dissolved in places and likely to be responsible for localized high groundwater salinities). This formation has a low permeability and acts as a confining layer capping the Penrith Sandstone. The outcrop of the Eden Shale occupies the centre of the Eden Valley syncline. The St Bees Sandstone formation conformably overlies the Eden Shale formation. This formation consists mainly of very fine to fine-grained, indurated sandstone. Mudstone beds are generally subordinate, though increase in abundance towards the boundary with the underlying Eden Shale formation (Stone et al., 2010).

Over three quarters of the Eden catchment bedrock geology is covered by Quaternary superficial deposits (Figure 3). Extensive areas of exposed bedrock are mainly restricted to the Lake District, the

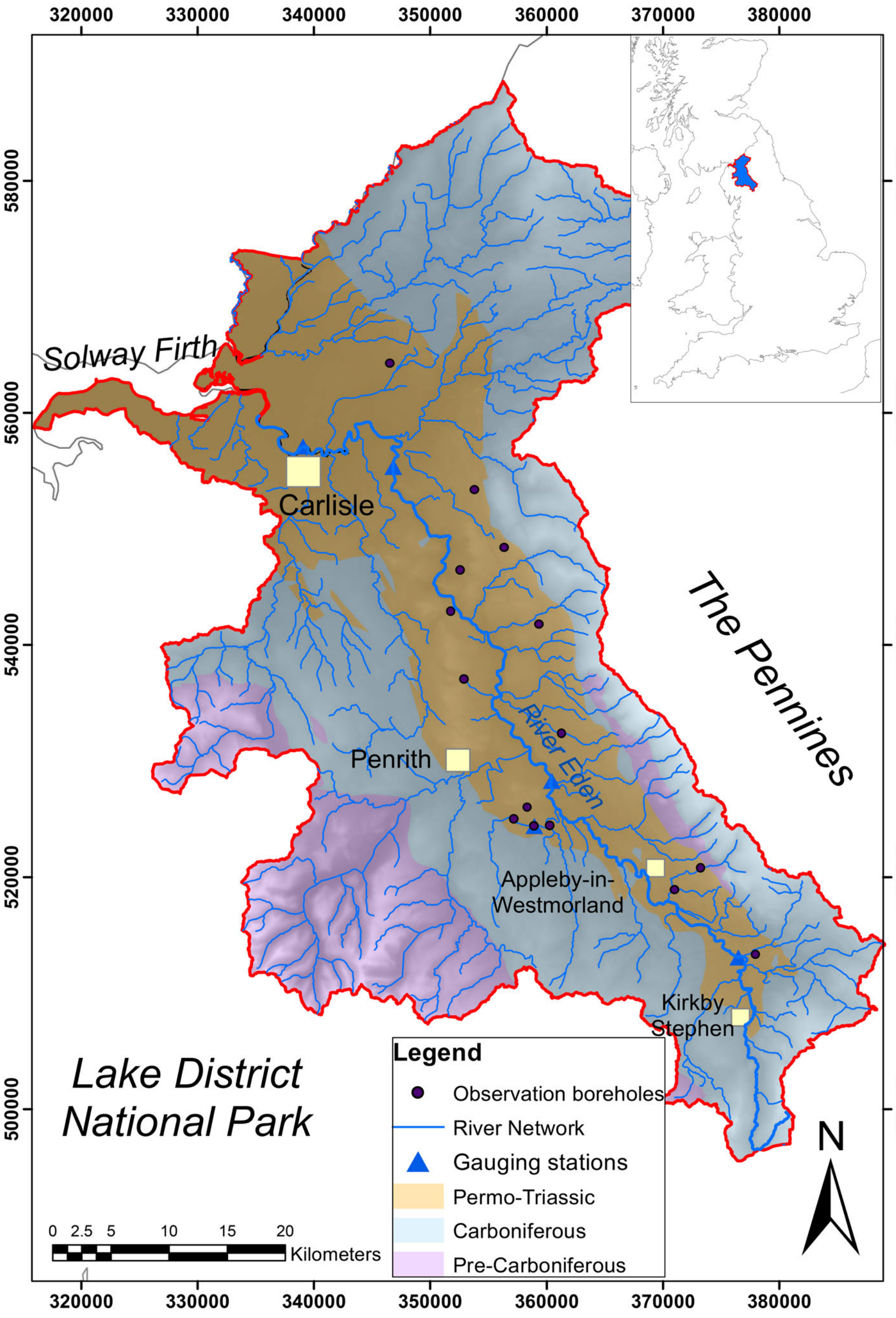

FIGURE 2 Geology of the Eden catchment

Northern Pennine escarpment and the outcrop of the Great Scar Limestone Group. Nevertheless, exposed areas of sandstone ('drift windows') are present, mainly in the southern part of the catchment. The stratigraphy of the superficial deposits is complex, with inter-digitations of sand, gravel, silt and clay that may each develop their own piezometric levels, resulting in complex perched water tables above the bedrock formations (Allen et al., 1997).

The Penrith and St Bees Sandstones are considered as the major aquifers in the Eden Valley (Table 1). They are characterized by moderate-high permeability and porosity. The Penrith Sandstone displays both vertical and horizontal heterogeneity (in terms of cementation and grain size), however the St Bees Sandstone tends to be more homogeneous and likely to behave as one aquifer. The hydrodynamic properties of both sandstones are summarized in Table 1 of Lafare et al. (2016), which uses core data from Allen et al. (1997). Generally, the regional groundwater flow is dominated by intergranular flow whilst flow into boreholes is predominantly contributed through fractures, which are only locally inter-connected (Allen et al., 1997). There are very limited pumping test data for the St Bees Sandstone Formation in the Eden Valley indicating transmissivity values ranging from 167 to 276 m^2/day. In the Penrith Sandstone Formation the transmissivities from 15 different pumping test sites range from tens of m^2/day to nearly 2000 m^2/day locally in the area of Cliburn, with a geometric mean of 390 m^2/day (Allen et al., 1997). The sandstone aquifers are covered by superficial deposits of variable lithology and thickness (up to 30 m in the northern part of the Eden catchment). It

TABLE 1 Simplified stratigraphic table (based on http://nora.nerc.ac.uk/id/eprint/12788/1/OR10063.pdf)

Age	Geology	Aquifer
Quaternary	Alluvium	Minor
	River Terrace Deposits	Minor
	Glacial Till	No
Tertiary	Mercia Mudstone	No
	Kirklinton Sandstone	Major
	St. Bees Sandstone	Major
Permian	Eden Shales	No
	Penrith Sandstone and Brockram	Major
Carboniferous	Pennine Coal Measures	Minor
	Yoredale	Minor
	Great Scar Limestone	Minor

seems likely that these deposits will have a significant impact on recharge and its distribution (Butcher et al., 2006).

The Permo-Triassic sandstones lie in a shallow synclinal structure aligned along the Eden valley. Where exposed they have been found to be heavily faulted though the superficial deposits probably limit the observation of much of the faulting. However, its impact on the groundwater flow system may be important especially in areas where silicification is found.

The principal aquifer types within the Eden catchment are fourfold:

1. Unconfined sandstone with little or no superficial deposit cover.
2. Unconfined sandstone covered by superficial deposits (>5 m thick) and an unsaturated zone within the sandstone.
3. Confined sandstone with groundwater levels that fluctuate within superficial deposits.
4. Limestone exhibiting significant fracture flow, with potentially enlarged fractures.

The surface water flow in the Eden catchment is derived from rivers flowing from adjacent uplands (Carboniferous Limestone and older formations), direct runoff within the Eden Valley and base flow contribution from the Permo-Triassic sandstone aquifers and other secondary aquifers.

Daily groundwater level time series are available from 18 boreholes, drilled into the Permo-Triassic Sandstones for a time period between 2000 and 2012, were obtained from the Environment Agency of England. They have been used for this study and their locations are presented in Figure 3. Further details of the boreholes and their setting can be found in Lafare et al. (2014). Figure 4 shows the normalized groundwater level time series plotted for each of these 18 boreholes. Of these boreholes 12 are in the Penrith Sandstone and 6 in the St Bees Sandstone (Lafare et al., 2014). It can be seen that the hydrographs from the different observation boreholes provide a variety of groundwater level responses in terms of shape and amplitude. Geographical, geological and hydrogeological information was collated and used to provide a qualitative description of the setting for each borehole. This information is summarized in Table 2 along with metrics and parameters related to the subsequently described modelling approaches.

2.3 | Modelling approach adopted

Time series of daily groundwater level fluctuations have been obtained for 18 boreholes in the Permo-Triassic sandstones of the Eden Valley. These hydrographs show a range of behaviours and therefore have been studied using statistical and time series analysis techniques (Lafare et al., 2016). Several characteristic behaviours have been identified and related to the geological and hydrogeological setting of each borehole. In this study, a range of lumped groundwater level time series modelling techniques are implemented and tested using the same data set, with the aim of assessing which modelling approach, which structure and which parameterization is the most suitable for simulating each characteristic behaviour. To achieve this, AquiMOD models have been calibrated to the groundwater time series, the IRF approach has been applied and finally, a combined IRF-AquiMOD approach is implemented which allows input stresses (rainfall, potential evaporation [PE] and river stage) to be used to define the IRF. These approaches are described in turn below.

2.4 | AquiMOD lumped groundwater level time series modelling

The AquiMOD model code has been developed and applied to various sites in the United Kingdom (Mackay et al., 2014a, 2014b). A summary is provided below for completeness, but further details are available in Mackay et al. (2014a, 2014b) and its application for seasonal forecasting is found in Mackay et al. (2015). AquiMOD consists of three basic elements: soil, unsaturated zone and the saturated zone, as described below:

1. Soil processes – recharge: The modified FAO method (Griffiths et al., 2008) is used to calculate recharge from the soil zone on a daily basis.
2. Unsaturated zone (UZ): Flow through the unsaturated zone is modelled either as a by-pass flow (no UZ) or using a Weibull distribution function to allow for the delay and attenuation of the soil discharge (recharge) in its passage to the saturated zone.
3. Saturated zone – different possible model structures are available: The basic unit of the saturated zone is the single ‘block’ with a head-dependent outflow. The block can consist of up to three layers with different transmissivity and or hydraulic conductivities and thicknesses, elevation of outflow and storage coefficients, including specific yield for the uppermost layer. A single block with a single transmissivity can also be used. A varying number of layers within the blocks can be used to test the effect of a variety of model structures on the hydrograph response.

The results are assessed by fitting to observed groundwater level fluctuations, numerically using the Nash Sutcliffe Efficiency (NSE)

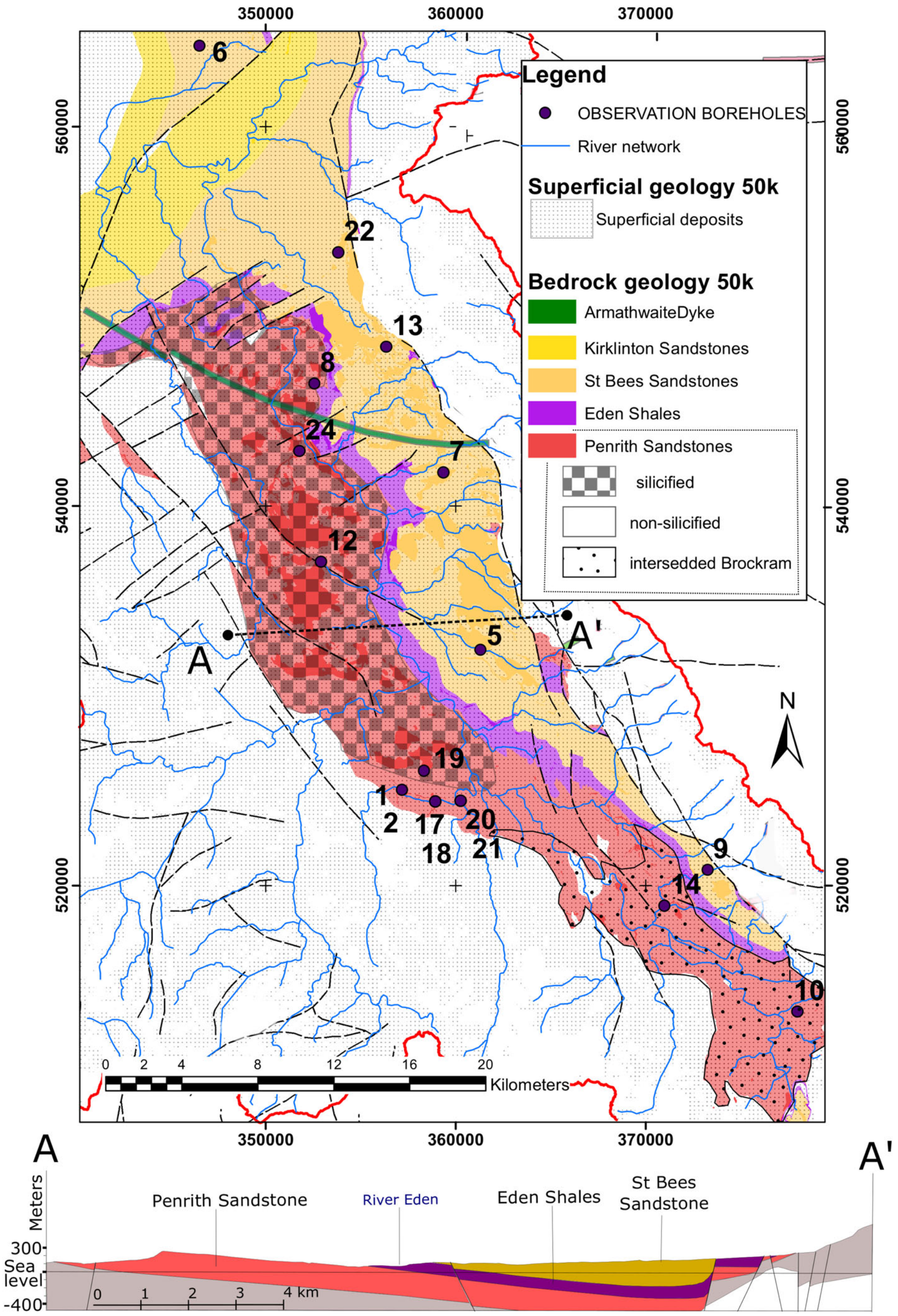

FIGURE 3 Location of boreholes used for the study

criterion and graphically. Monte Carlo simulations are also used to identify, where possible, more focused ranges for the various parameters. The best model structures and parameter sets are identified for each borehole hydrograph. The identifiability of the structures and parameters sets is assessed and a first attempt at classification is proposed.

2.5 | Impulse response functions: Basic application

In order to assess and/or refine the previously proposed classification, an IRF methodology was applied, to obtain a fit to the observed daily groundwater level fluctuations using rainfall and the temperature as driving variables. The model comprises the simulation of two processes in series. The first is the process of generating recharge from precipitation; the second is recharge entering storage and causing a system response like groundwater head change. The methodology here is based on the Rainfall-Response Aquifer and Watershed Flow Model (RRAWFLOW; Long, 2015), a lumped model that is partially based on unit-hydrograph theory applied to streamflow. The model simulates a time-series record for a measurement point of streamflow, spring flow, groundwater level, or solute transport in response to a system input of precipitation, recharge, or solute injection.

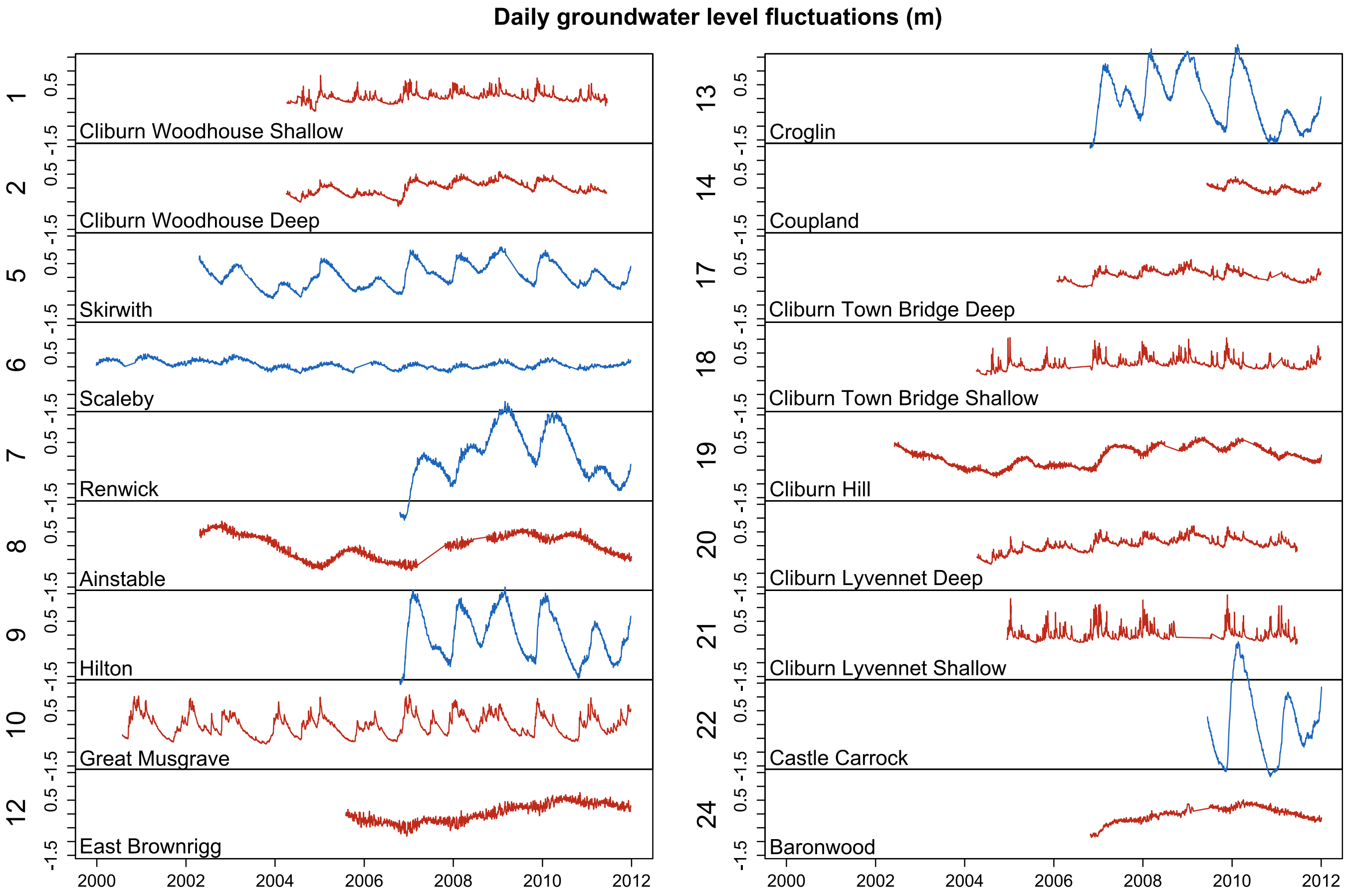

FIGURE 4 Normalized hydrographs for 18 boreholes used in the study

The recharge calculation for this method is described in Long and Mahler (2013). The convolution is a time-series operation that is commonly used in non-distributed hydrologic models to simulate streamflow, spring flow, or groundwater level in response to recharge. The use of convolution in modelling also has been described as a linear reservoir model and a transfer-function model. The discrete form of the convolution integral for uniform time steps used here is:

$$y_i = \Delta t \sum\nolimits_{j=0}^{i} \beta_i h_{i-j} u_j + \varphi_i + d_0; i,j = 0,1,\ldots,N, \qquad (1)$$

where h_{i-j} is the IRF, u_j is the input or forcing/stress function; j and i are time-step indices corresponding to system input and output, respectively; N is the number of time steps in the output record; β_i is an optional time-varying IRF scaling coefficient; φ_i represents the errors resulting from measurement inaccuracy, sampling interval, or simplifying model assumptions; and d_0 is a hydraulic-head datum, namely the level to which hydraulic head would converge if the local recharge was eliminated (Long, 2015). The difference between i (output time step index) and j (input time step index), that is $i - j$, represents the delay time from impulse to response, and the IRF represents a distribution of these delay times. The input function is, in this case, the recharge, and the system response the groundwater level fluctuations. The IRF of the hydrologic system is approximated by a parametric function: the gamma function, equivalent to the Pearson type III function:

$$\gamma(t) = \frac{\lambda^{\eta} t^{\eta-1} e^{-\lambda t}}{\Gamma(\eta)}; \lambda, \eta > 0, \qquad (2)$$

$$\Gamma(\eta) = \int_{t=0}^{\infty} t^{\eta-1} e^{-t} dt, \qquad (3)$$

where λ and η are non-dimensional shape parameters. The equation is approximated in RRAWFLOW by the discrete form:

$$\Gamma(\eta) = \Delta t \sum\nolimits_{t=t_0}^{\infty} t^{\eta-1} e^{-t}, \qquad (4)$$

where t is time centred on each discrete time step, t_0 and N are time centred on the initial and final time steps, respectively, and Δt is the time step duration (Long, 2015). An additional scaling coefficient ε is introduced for increasing the range of hydrological applications:

$$h(t) = \varepsilon \gamma(t), \qquad (5)$$

where ε (non-dimensional) compensates for hydrological systems that do not have a one-to-one relation between system input and output

TABLE 2 Summary of AquiMOD results

Observation borehole			Bedrock	Superficials		Model type		Performance		Soil component					Unsaturated			Saturated							
No	Name	Code	Formation	Type	Thickness (m)	Run	Nb of layers	NSE cal	NSE eval	Field capacity (m)	Wilting point (m)	Max root depth (mm)	Depletion factor (–)	BFI (–)	k (m/d)	Lambda (–)	n (–)	Aquifer length (m)	S (–)	K3 (m/d)	K2 (m/d)	K1 (m/d)	Z3 (m ASL)	Z2 (m ASL)	Z1 (m ASL)
8	Ainstable	54/10	Penrith	Till	17	2	3	0.527578	0.362872	0.2857	0.185	3705.77	0.535576	0.458931	9.40782	9.61107	32.5734	3500	0.169111	40.9038	27.6902	0.287691	84.0715	80.3012	-5
24	Baronwood	54/56	Penrith	Sand gravels	3	4	3	0.864	0.296213	0.2857	0.185	2744.99	0.946753	0.518296	7.29701	7.53349	55	1500	0.435937	43.6318	83.9123	0.007104	85.2978	83.0685	6.48
22	CastleCarrock	55/71	St Bees	Glacio fluvial	3	2	1	0.930189	0.687407	0.2857	0.185	955.26	0.087492	0.423035	9.06146	19.9277	55.7106	2500	0.021604	-	-	0.629675	-	-	79.02
19	CliburnHill	52/2H	Penrith	Sand	2	2	3	0.813572	0.357436	0.2857	0.185	3452.39	0.972833	0.567528	1.18622	9.74264	53.4356	600	0.313642	90.3968	53.4609	0.007104	112.679	110.509	70
21	CliburnLyvennet1S	62/40	Penrith	Alluv.	3	1	3	0.806098	0.778751	0.2857	0.185	833.995	0.283839	0.538768	1.06098	14.536	17.3136	288.092	0.446838	91.2817	39.8357	0.004052	106.824	106.341	56
20	CliburnLyvennet2D	62/41	Penrith	Alluv.	3	2	2	0.825635	0.783125	0.2857	0.185	500	0.730098	0.420499	2.43129	3.58354	20	600	0.379534	-	89.3888	0.013052	-	106.2	56
18	CliburnTownBridge1S	52/25	Penrith	Alluv.	1.5	3	2	0.630392	0.663655	0.2857	0.185	539.927	0.62533	0.434083	-	-	-	100	0.053502	-	55.0646	0.001	-	109.816	101.874
17	CliburnTownBridge2D	52/26	Penrith	Alluv.	1.5	3	2	0.841203	0.70976	0.2857	0.185	478.646	0.462151	0.4373	-	-	-	200	0.343023	-	50.2976	0.004052	-	110.42	64
1	CliburnWoodhouse1S	52/23	Penrith	Alluv.	2	3	2	0.673108	0.632605	0.2857	0.185	465.493	0.831547	0.644542	-	-	-	100	0.244075	-	76.2324	0.0001	-	116.338	107
2	CliburnWoodhouse2D	52/24	Penrith	Alluv.	2	3	2	0.932515	0.865016	0.2857	0.185	960.796	0.293021	0.663988	-	-	-	200	0.382237	-	77.8833	0.007104	-	116.223	67.15
14	Coupland	71/23	Penrith	Sandy clay	5	3	3	0.877869	0.40331	0.2857	0.185	567.019	0.907483	0.507993	-	-	-	1000	0.348216	9.39961	90.3144	0.03457	135.869	134.011	58
13	Croglin	54/54	St Bees	-	-	4	2	0.808263	0.630714	0.2857	0.185	2000	0.725134	0.421235	1.02087	10.8381	50	1500	0.027195	-	95.2147	0.18699	-	166.503	118.03
12	EastBrownrigg	53/9	Penrith	Till	10	4	3	0.639515	0.49109	0.2857	0.185	4753.76	0.165253	0.462685	34.2907	191.797	149	7000	0.297397	46.7579	35.7494	11.839	104.624	103.888	69.2
10	GreatMusgrave	71/3	Penrith	Till	24	3	2	0.850018	0.85523	0.2857	0.185	670.846	0.798109	0.475832	-	-	-	300	0.065046	-	83.9383	0.0001	-	151.694	49.6
9	Hilton	72/9	St Bees	Till	11	2	2	0.940876	0.940874	0.2857	0.185	2500	0.114439	0.546965	1.83444	10.4873	50	1500	0.053485	-	40.8458	0.147487	-	213.061	138.97
7	Renwick	54/55	St Bees	Sand gravels	3	4	3	0.764828	0.469897	0.2857	0.185	4116.95	0.240352	0.550932	9.64019	15.193	21	2000	0.075035	90.2717	79.1	0.150539	175.995	175.055	102.4
6	Scaleby	46/3	Kirklinton /St Bees	Till	13	3	2	0.82073	0.208516	0.2857	0.185	2617.28	0.471333	0.502438	-	-	-	3500	0.292328	-	4.33153	5.15467	-	40.8521	−30
5	Skirwith	63/2	St Bees	Till	3	1	2	0.902584	0.902448	0.2857	0.185	4000	0.986142	0.481961	3.83538	5.56276	133.675	764.061	0.088763	-	60.6376	0.007104	-	129.4	35

Darker green = higher NSE and better calibration Darker orange = lower NSE and poorer calibration.

(as for recharge and groundwater level fluctuations). An important feature of RRAWFLOW is the possibility of using up to two superimposed gamma functions: allowing either to represent quick flow and slow flow/conduit and diffuse flow. Each parametric function represents one of the two flow components. This feature is used here to identify the borehole hydrographs that are better reproduced using a representation with more than one flow component. Moreover, different IRFs are considered for dry and wet periods within the simulation period (these periods are determined using a moving average of the rainfall).

Using a combination of manual trial-and-error and automatic optimisation based on the Monte Carlo approach (Hill & Tiedeman, 2006), the IRF parameters were fitted in order to produce a good fit to the borehole hydrographs. A single IRF was first considered, and its parameters fitted. This allowed the range of parameters used as input for the optimisation process to be reduced, and to include a second IRF. The resulting IRF for each borehole was then extracted, plotted, and described using a number of metrics. These metrics were chosen to quantify a number of characteristics of the IRF shapes. To define these metrics, the IRF was assumed to be a frequency distribution of the transit times of the response (hydraulic head). The selected metrics quantify the IRF shape independently from the scale so that comparisons are not weighted by IRF amplitude (which can vary from one location to another). Therefore, a number of ratios are calculated. The metrics included two scale-independent moments, skewness and kurtosis, and five ratios: standard-deviation/mean, standard-deviation/memory, mean/memory, mode/memory, peak-height/area. These seven metrics were quantified for wet and dry periods separately, resulting in 14 metrics. These metrics are tabulated along with the general shapes of the optimized IRF, allowing comparison of the results for each borehole, and a new classification to be proposed.

2.6 | AQUIMOD-IRF: Impulse response functions using different stresses

The modelling approach described above allows the identification of whether a particular groundwater level fluctuation behaviour requires the combination of two (or more) IRFs to obtain a reasonably good fit. This methodology was extended to use IRF to simulate groundwater level fluctuation, using rainfall, potential evapotranspiration (PE) and surface water level (river stage) as driving variables. Indeed, such a modelling approach has been shown to be able to decompose series of groundwater level fluctuations into partial components, each representing the contribution of an individual stress. Here the objective was to evaluate the potential impact of the local surface water level variation (river stage) on the groundwater level fluctuations.

This method used here is based on the work presented by von Asmuth et al. (2008) and involves the implementation of a time series modelling approach that aims to reproduce groundwater head fluctuations subjected to multiple stresses. Using predefined IRFs, multiple stresses that may influence groundwater level fluctuations can be taken into account. Each stress has a specific parametric IRF and related parameters.

Here we use three different stresses represented by input time series: the rainfall time series, the PE time series, and the local surface water level time series. Further explanation of the mathematics of the approach is given in Appendix A. This methodology was incorporated into the AquiMOD code by adding an IRF approach to each of the soil moisture, unsaturated zone and saturated zone components. For each time step the input from each stress was combined to produce a single groundwater head. The results reported here use the IRF approach for the saturated zone to integrate the stresses on a time series basis together with recharge from the unsaturated zone to create a time series of groundwater heads.

To calibrate the model, Monte Carlo simulation was performed using an initial range of parameters, for all the boreholes. An initial fit, using only the climatic stresses (rainfall and evaporation) was obtained. This allowed a reduction in the range of parameters of the climatic IRF θ_p (see Equation (A4)) and the parameters produced which scale the evaporation (i.e. f in Equation (A3)). Using the reduced initial ranges, a second Monte Carlo run was carried out, this time including the surface water level stress and the associated IRF. In this way, the contribution of the surface water level stress to the improvement of the fit to the groundwater level fluctuations could be assessed. The boreholes for which the surface water level has a significant influence were then identified.

3 | RESULTS

The results are described and discussed first separately for each method used, and then summarized and discussed as a whole. The first application of AquiMOD to simulate the borehole response is described, then the single and double responses and finally the double response function with stresses are presented.

3.1 | Application of AquiMOD

A number of model structures have been tested; these include varying the number of layers for the saturated zone from one to three, as well as the inclusion or absence of an Unsaturated Zone. The results are summarized in Table 2 for the best-fit model (highest NSE) for each AquiMOD model. Table 2 presents the best model structures and parameters sets for each borehole. The NSE for the best model for both calibration and evaluation are presented. In general, the NSE is higher for boreholes within the St. Bees and shows less consistency between calibration and validation for the Penrith sandstone boreholes. The NSE for the evaluation period is particularly poor for Ainstable (54/10), Baronwood (54/56), Cliburn Hill (52/2H), Coupland (71/23), East Brownrigg (53/9), Renwick (54/55) and Scaleby (46/3). Some of this poor performance can be explained by the short data periods, for example Coupland and Renwick. It is also possible to improve the fit by removing the Unsaturated Zone components for the shallow boreholes situated on the banks of the River Leith, that is numbers 17/18 and numbers 20/21. However, in general it is more difficult to identify a model structure that reproduces effectively the hydrographs for the boreholes drilled in the Penrith sandstone. It is, therefore, necessary to understand what processes can be contributing to this failure to reproduce the hydrographs with the model.

Given that the best fit, consistently good for the calibration and the validation period, was obtained for the boreholes drilled into the St Bees sandstone formation, an example of the match obtained between modelled and observed is presented for the Hilton OBH (No. 9) which has a NSE of 0.94 for both calibration and validation (Figure 5). To illustrate the identifiability or otherwise of the parameters obtained during calibration, an example of a sensitivity analysis is presented (Figure 6).Specific yield shows identifiability and these are consistent between the fitted parameters (and model structures) for most of the St Bees boreholes. The exception is Scaleby, No. 6, which is situated in the north, on the outcrop of the Kirklinton sandstone, which is more silicified than the St. Bees sandstone, so represents a significantly different lithology.

It appears that to simulate the borehole response for the Penrith sandstone a different approach is required to that of just using AquiMOD as a lumped parameter groundwater model. The methods used to investigate the flow processes that could be operating, but which may not be able to be simulated by a lumped model are, therefore, described in the following section.

3.2 | Single, double impulse response function

Table 3 summarizes the IRF metrics and IRF response curves for the various boreholes. They show a general pattern for each type of observation borehole setting:

1. A single IRF with a relatively long tail and a slightly delayed peak is usually obtained to reproduce the hydrographs of the St Bees sandstone, for example Croglin (No. 13).
2. A double IRF is consistently needed for simulating the hydrographs of the silicified Penrith sandstone: a sharp and nearly immediate peak, followed by a significantly delayed (10 months or more) peak, spread over a long period (months) and with a long tail, for example Baronwood (No. 24).
3. A double IRF is generally needed for the central Penrith sandstone outcrop (banks of the River Leith), for example Cliburn Townbridge (No. 17): a sharp and immediate peak (usually more intense in the case of the shallow boreholes); a delayed and more widely spread peak, of various shapes which varies from one borehole to another (see Table 3).

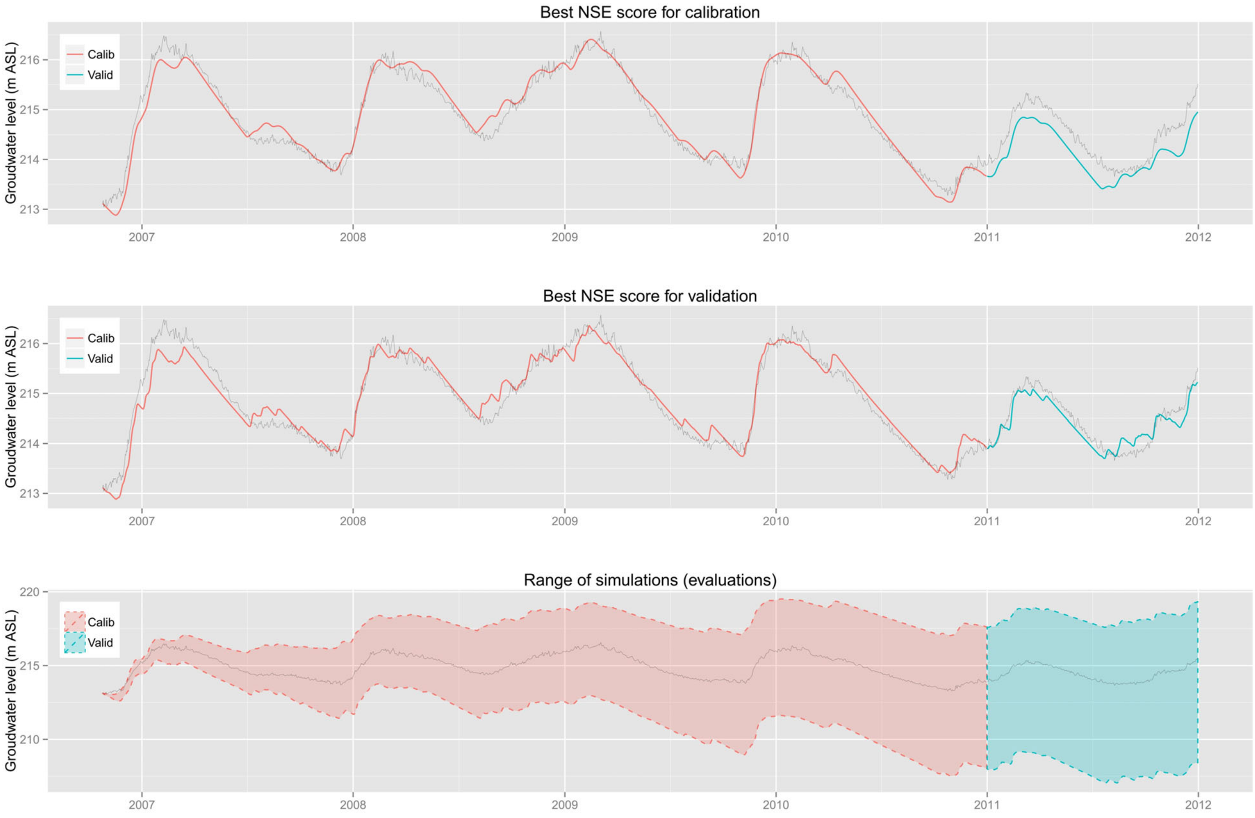

FIGURE 5 Comparison of observed and hydrograph and AquiMOD model output for best Nash Sutcliffe Efficiency (NSE) for calibration and validation at Hilton (No. 9; St. Bees)

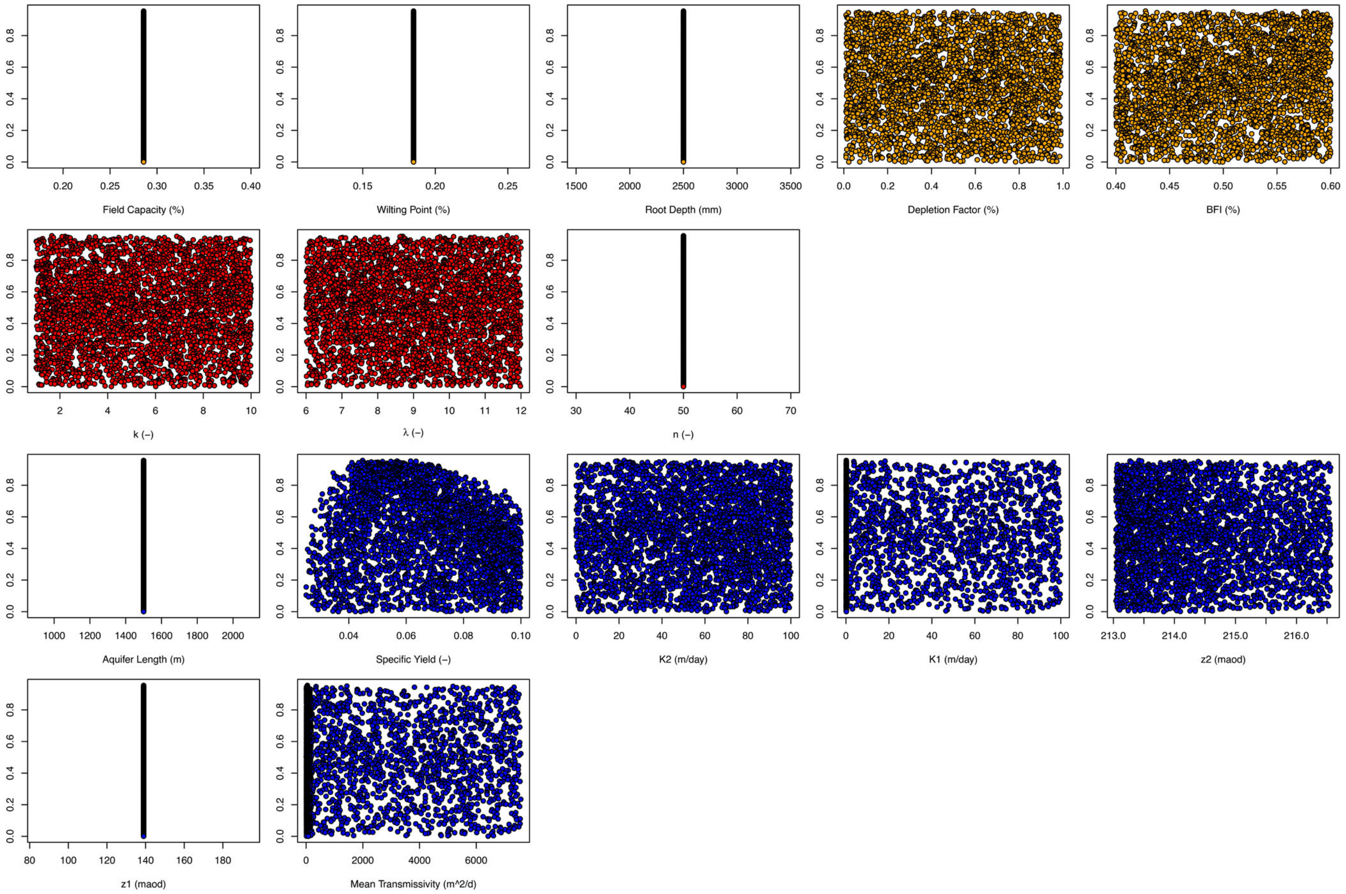

FIGURE 6 Identifiability using Nash Sutcliffe Efficiency (NSE) of Hilton AquiMOD model

4. A single IRF with an exponentially decreasing shape is obtained for the two boreholes situated in the Brockram at the base of the Penrith sandstone, for example Coupland (No. 14).

As mentioned earlier this work is an extension of that presented by Lafare et al. (2016) where three types of aquifer response were identified by correlation analysis: Northern Penrith, Southern Penrith and St. Bees.

Figures 7–9 show examples of groundwater level fluctuation fitting, with the shapes of the optimized IRF for Cliburn Townbridge (No. 17), East Brownrigg (No. 12) and Skirwith (No. 5).

Cliburn Townbridge (Figure 7) exhibits a double IRF both of which have a peak within a short time interval (~1 day) and then a decay. One of the IRF curves has a second peak around 200 days. This demonstrates two relationships: a fast flow component and a second, longer timescale component. The fast flow component provides the flashy part of the hydrograph (fracture flow or the influence of the river) whilst the longer time input demonstrates the inter-annual variation (water provided from storage within the sandstone).

East Brownrigg (Figure 8) has a double IRF again similar to Cliburn Townbridge which had a peak within a short time interval and then both with secondary peaks one after ~200 days and the other after 600 days. Whilst the short timescale peaks produce subdued flashy response the later peaks provide the inter-annual variation.

Skirwith (Figure 9) has two IRF curves with single peaks both after ~50 days. This configuration of the IRFs results in a very smooth response with little or no flashiness.

To investigate how surface water flows and levels can influence groundwater response more fully the stress related IRF was implemented.

3.3 | AQUIMOD-IRF: Stress related double impulse response functions

Figures 10–12 show examples of fitting, IRF shapes and contribution of each simulated stress for the Brockram Penrith sandstone boreholes. The results for Great Musgrave (Figure 10) are taken as an example, as there is a gauging station close by (River Eden at Great Musgrave Bridge) with a long record of river stage. The fitting is slightly better in terms of NSE compared to the AquiMOD model and the timing and amplitude of the peaks are well represented; the river stage contribution is particularly useful for simulating accurately the higher peaks. In boreholes drilled in the central Penrith sandstone (e.g. Cliburn Lyvennet [shallow]; Figure 11) the fit is consistently

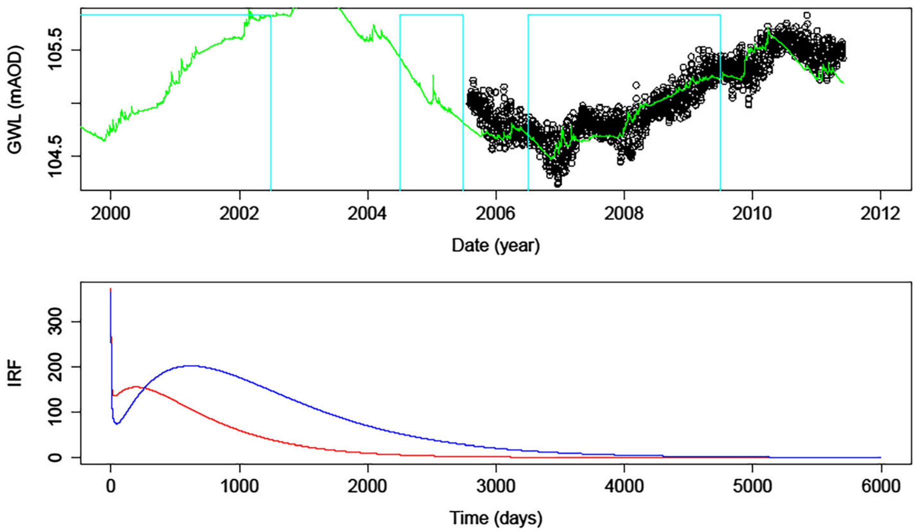

FIGURE 7 Modelled groundwater level (GWL) hydrograph using impulse response function (IRF) for Cliburn Townbridge (BH No. 17); green line simulated; black dots observed

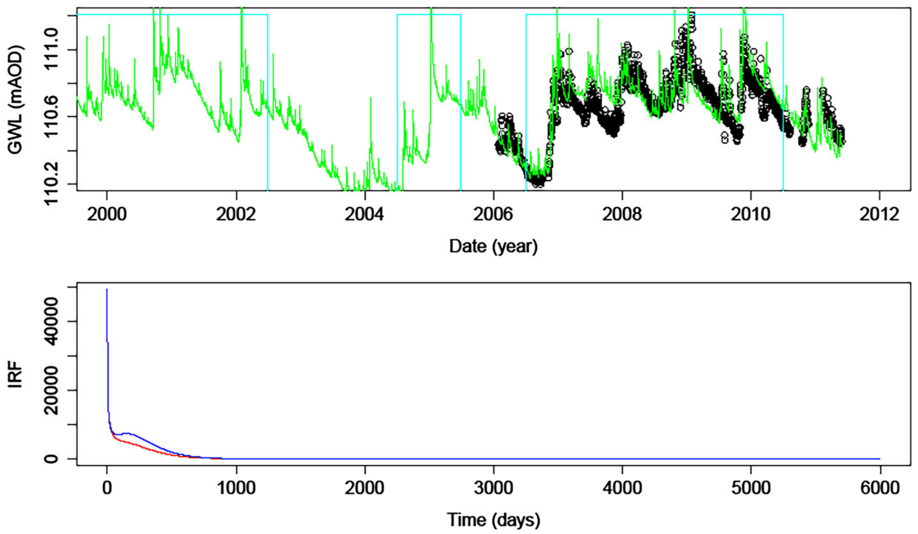

FIGURE 8 Modelled groundwater level (GWL) hydrograph using impulse response function (IRF) for East Brownrigg (BH No. 12); green line simulated; black dots observed

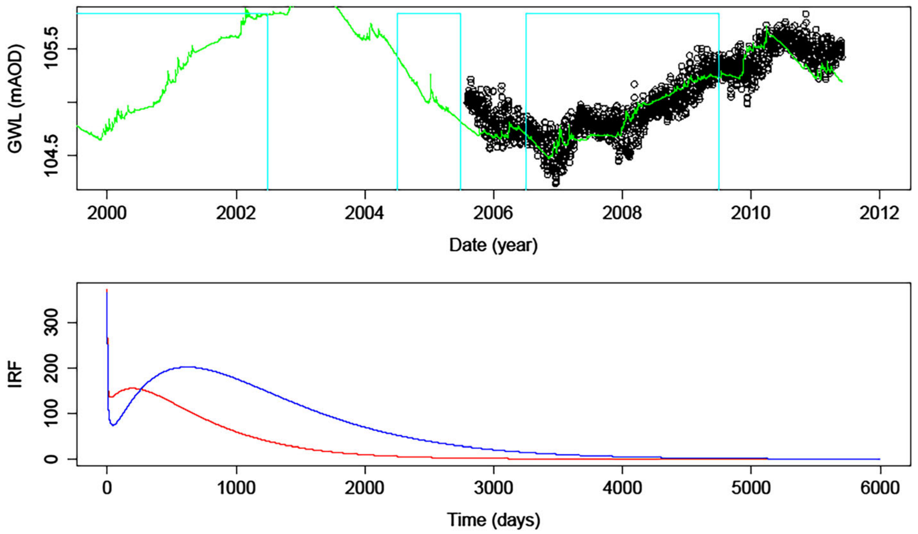

FIGURE 9 Modelled groundwater level (GWL) hydrograph using impulse response function (IRF) for Skirwirth (BH No. 5); green line simulated; black dots observed

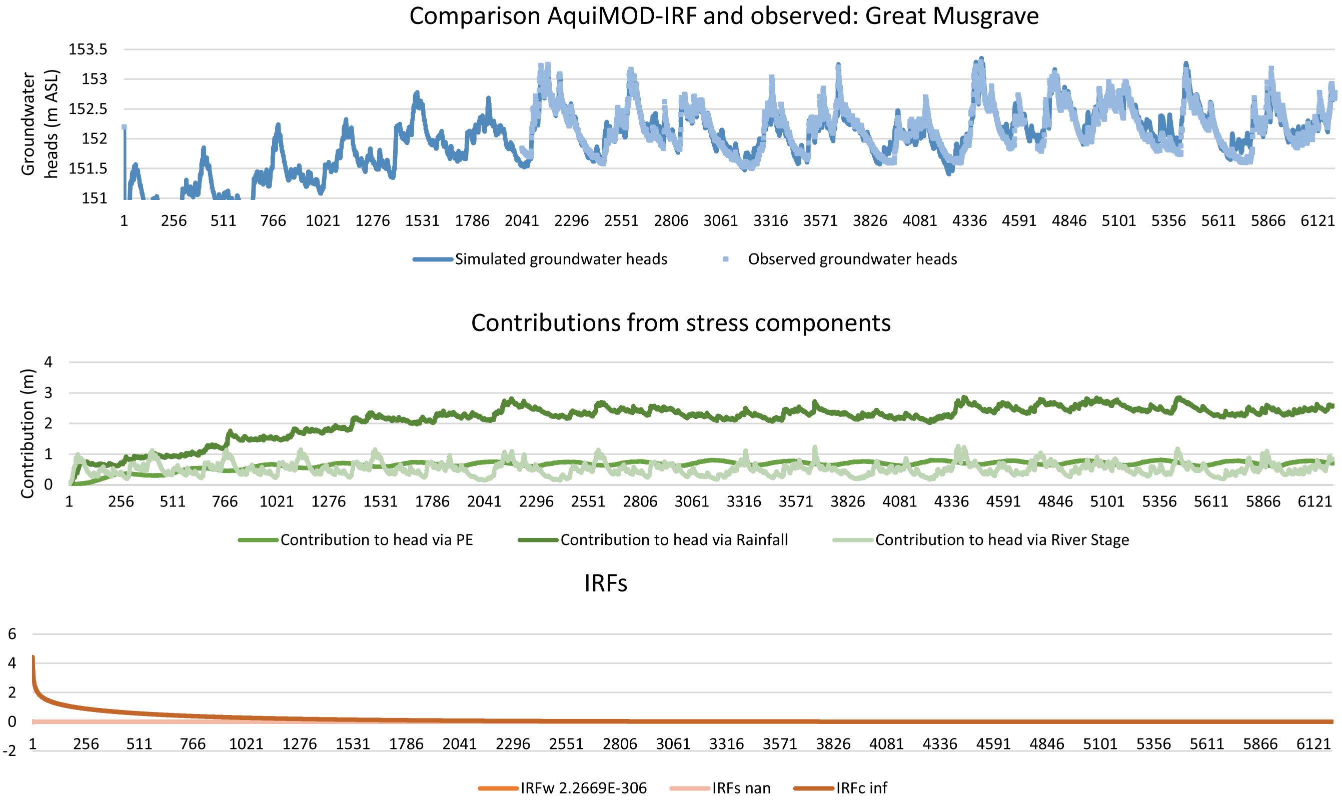

FIGURE 10 Modelled hydrograph using stress impulse response function (IRF) for Great Musgrave

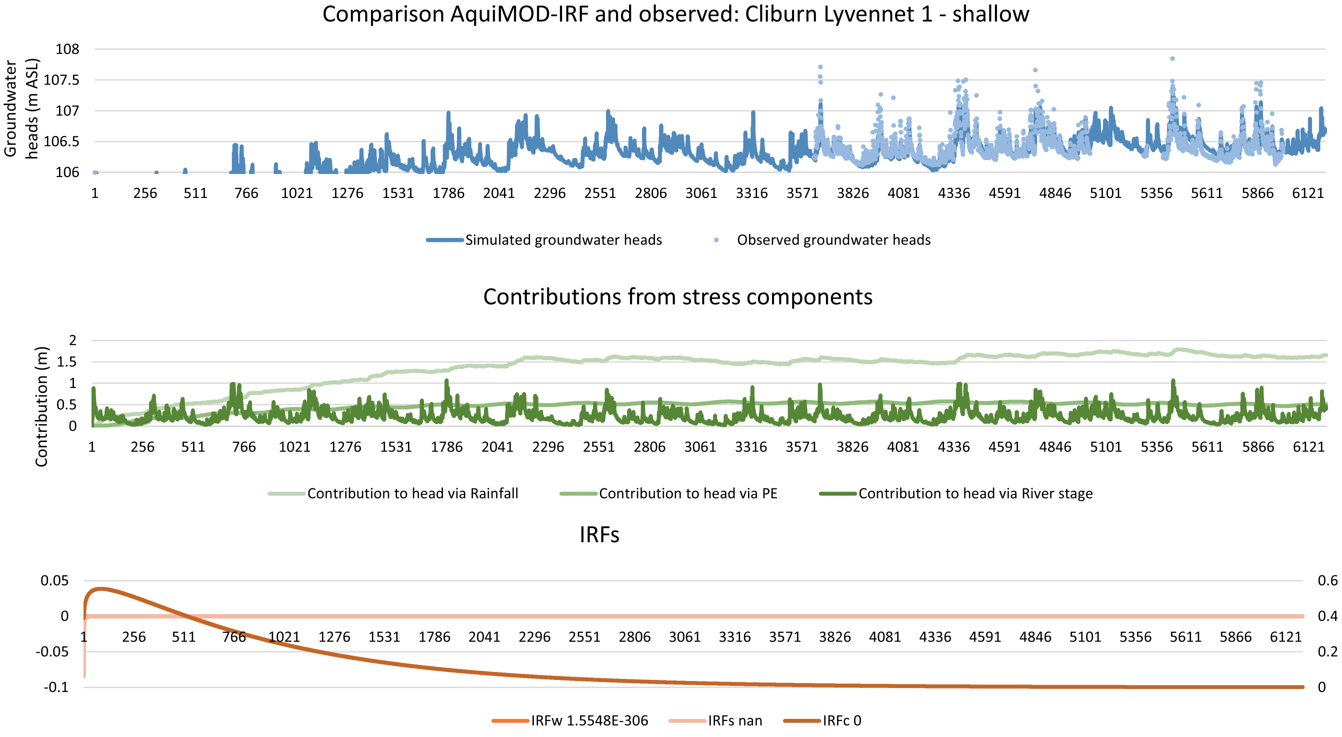

FIGURE 11 Modelled hydrograph using stress impulse response function (IRF) for Cliburn Lyvennet

better when the IRF is introduced to the AquiMOD code even though the river stage is recorded at the Temple Sowerby gauging station on the river Eden which is some distance from the boreholes. The impact of the river stage is more important for the shallow borehole than for the deep boreholes and the peaks are well reproduced. The Cliburn Woodhouse 2 (deep) borehole (Figure 12) does not show a significant

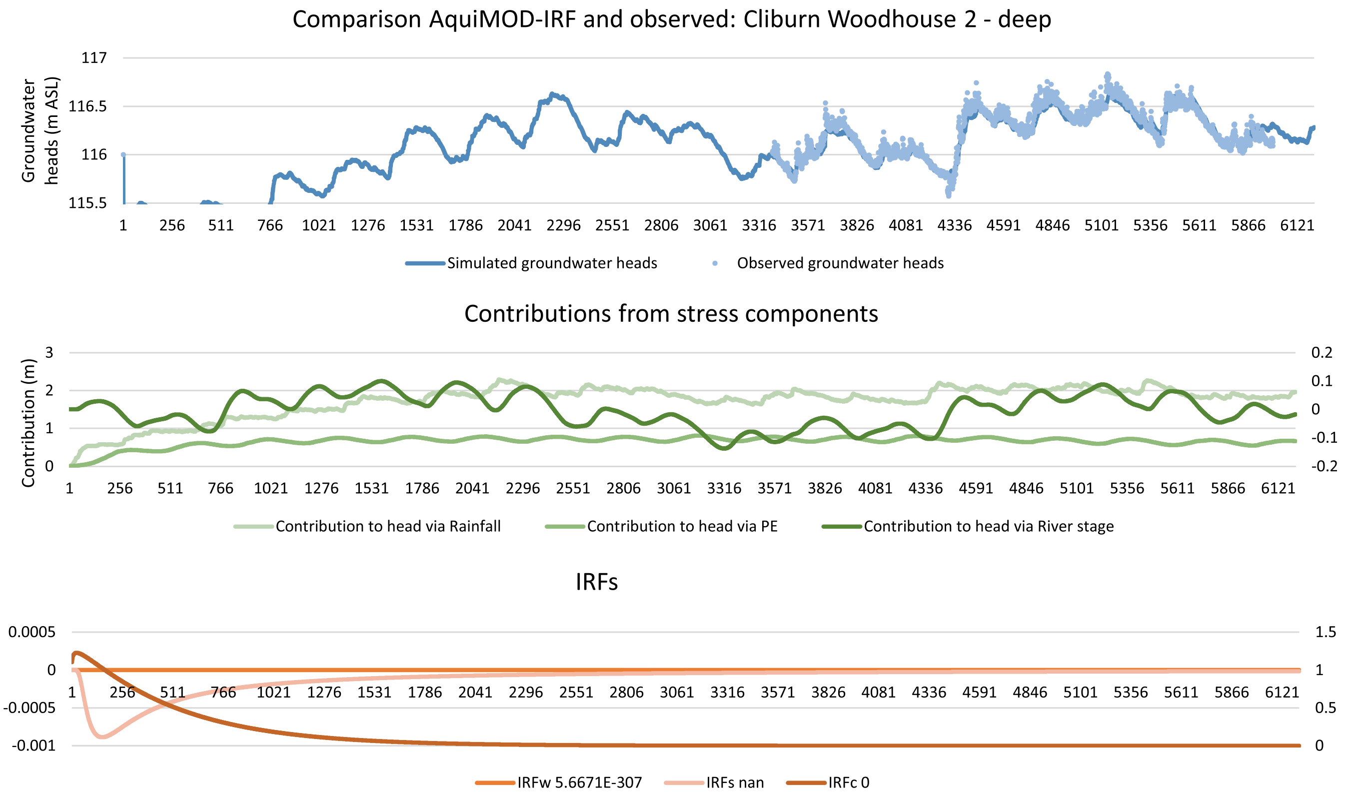

FIGURE 12 Modelled hydrograph using stress impulse response function (IRF) for Cliburn Woodhouse (deep)

contribution from the river stage component as evidenced by the lack of river stage (represented by h[s] on Figure 12) response function.

The stress-related IRF provides another way of decomposing a groundwater level fluctuation time series, and provides reliable information on the degree of connection between aquifers and surface water in this groundwater system.

3.4 | General discussion: Which modelling approach should we use depending on the shape/behaviour of the hydrograph?

Previous work on the Eden catchment (Lafare et al., 2016) used the Seasonal Trend analysis by Loess (STL) method to identify seasonality, trend and noise components for the groundwater hydrographs produced from the Eden boreholes. By examining the variance of these three different components two classes of response could be identified: namely Silicified Penrith Sandstone and the shallow boreholes around the River Leith. Further work using clustering analysis by principal component analysis (PCA) enabled the identification of groups in both the St. Bees Sandstone and the Penrith Sandstone. Using the IRF approach (Table 3) has extended this analysis to identify four types of hydrograph response associated with differing hydrogeological settings: (1) St. Bees Sandstone; (2) in the Brockram; (3) in the Silicified Penrith Sandstone; and (4) in the central part of the Penrith Sandstone heavily influenced by the interaction with rivers.

AquiMOD simulates the hydrograph response in the St. Bees sandstone well. It also performs well on those borehole hydrographs from the central Penrith Sandstone close to the rivers. However, there are problems in some of the simulations, particularly with the validation for the Silicified Penrith Sandstone (Ainstable, Baronwood and East Brownrigg). Examination of the IRF curves for these boreholes indicates that there is a fast flow response together with a longer-time response. The fast response is likely to represent fracture flow which AquiMOD is not designed to simulate. Similarly, some of the Penrith Sandstone time series, where they are close to rivers did not produce good results (Cliburn Woodhouse and Cliburn Townbridge). This is likely to be due to the aquifer here exhibiting dual fast and slow flow responses.

The poorest AquiMOD model results occurred when there are differences between the two seasonal IRF curves for each borehole, for example Baronwood, which suggests differing seasonal responses. As well as Baronwood, both Ainstable and East Brownrigg time series proved difficult to model and had the lowest NSEs for the AquiMOD modelling. This could perhaps be due to differing seasonal behaviour, due to changing saturation of the superficial deposits.

Lumped parameter models such as AquiMOD perform better when simpler IRF response are observed, that is single peak IRF curves that are similar between wet and dry periods. Complications such as twin peaks, very fast decay of the IRF curve or significantly different IRF curves between dry and wet periods are the most difficult for AquiMOD to simulate. It is suggested that a screening approach

TABLE 3 IRF summary statistics

IRF metrics	Single or double IRF		Skewness	Kurtosis	St. Dev / Mean	St. Dev / Memory	Mean / Memory	Median / Memory	Peak-Height / Area	Memory (days)	Peak time 1 (days)	Peak time 2 (days)	Peak time 2 (days)
Ainstable	D	Dry	3.811773	16.26352	3.198571	0.072839	0.022772	2.98E-15	1.96352	729	5	392	
		Wet	2.207652	3.683141	2.115303	0.127475	0.060263	6.97E-05	0.741545	1273	5	412	
Baronwood	D	Dry	3.191779	16.74836	2.153631	0.02976	0.013819	1.69E-04	1.520398	1403	5	210	
		Wet	1.44195	0.766887	1.504073	0.061237	0.040714	4.90E-03	0.495364	2163	5	464	
CastleCarrock	S	Dry	5.907844	35.83536	5.004916	1.168385	0.233447	5.89E-17	2.394712	284	41		
		Wet	5.357753	29.01736	4.635129	1.25574	0.270918	3.26E-17	2.014283	317	67		
CliburnHill	D	Dry	5.859627	36.4429	4.174246	0.035671	0.008546	0.00028	2.356452	999	12		
		Wet	3.623382	12.45	3.031058	0.052966	0.017474	0.00056	1.314339	995	1	143	
CliburnLyv1	D	Dry	40.12337	2198.995	16.73142	12.95278	0.774159	4.25E-38	66.37757	49	1		
		Wet	42.28624	2348.724	8.071925	7.868979	0.974858	0.001203	31.0917	906	1		
CliburnLyv2	D	Dry	6.528165	118.665	2.366028	0.465968	0.196941	0.009694	4.082894	1403	1	412	
		Wet	2.816709	10.36703	2.385847	1.059846	0.444222	6.41E-07	1.822271	972	1	438	
CliburnTB1	D	Dry	39.58325	1992.285	7.175745	0.543069	0.075681	1.11E-08	25.93333	876	1	401	
		Wet	33.19338	1584.627	5.04368	0.454074	0.090028	1.47E-08	17.07808	893	1	401	
CliburnTB2	D	Dry	10.48416	213.1313	4.134027	2.799762	0.677248	8.12E-07	7.969001	562	1		
		Wet	6.716376	94.64375	3.530848	3.437329	0.973514	8.12E-07	5.526105	588	1	146	
CliburnWH1	D	Dry	11.15138	175.7125	4.363495	0.484814	0.111107	2.18E-10	5.376113	593	3	201	
		Wet	11.15138	175.7125	4.363495	0.484814	0.111107	2.18E-10	5.376113	593	3	201	
CliburnWH2	D	Dry	13.15248	406.5819	1.912211	0.192783	0.100817	0.02256	4.557236	3173	1	469	
		Wet	2.659126	7.877488	2.066727	0.414088	0.200359	0.002023	0.993164	1466	1		
Coupland	S	Dry	7.454003	73.86359	4.527949	1.586427	0.350363	1.63E-06	5.316285	521	1		
		Wet	7.454003	73.86359	4.527949	2.37964	0.525545	2.44E-06	5.316285	521	1		
Croglin	S	Dry	3.997125	15.85757	3.309763	0.273585	0.08266	1.44E-06	1.180799	676	41		
		Wet	3.515045	11.72645	3.030656	0.352104	0.116181	3.59E-06	0.956423	748	81		
EastBrownrigg	D	Dry	1.913149	2.645781	1.793107	0.02518	0.014043	0.00076	0.906481	1783	1	196	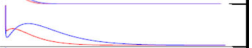
		Wet	0.970095	-0.5178	1.18484	0.038009	0.032079	0.011443	0.389561	2894	1	621	
GreatMusgrave	S	Dry	7.454003	73.86359	4.527949	6.345708	1.401453	6.51E-06	5.316285	521	1		
		Wet	7.454003	73.86359	4.527949	7.932135	1.751816	8.14E-06	5.316285	521	1		
Hilton	S	Dry	4.283402	18.34627	3.566241	0.146853	0.041179	5.20E-08	1.331873	578	42		
		Wet	3.835418	14.72128	3.096767	0.169777	0.054824	1.10E-05	1.104672	798	26		
Renwick	S	Dry	3.137397	8.889023	2.823386	0.056556	0.020031	2.68E-07	0.80638	797	161		
		Wet	2.521279	5.312203	2.233413	0.233479	0.104539	0.000935	0.570719	1296	116		
Skirwith	S	Dry	3.997125	15.85757	3.309763	0.125067	0.037787	6.57E-07	1.180799	676	41		
		Wet	3.835418	14.72128	3.096767	0.133998	0.04327	8.68E-06	1.104672	798	26		

undertaken by producing the IRF curves would then be able to identify the likelihood for a successful model calibration.

The shortcomings of the AquiMOD approach can be addressed using the time series IRF incorporated into the AquiMOD code structure (AquiMOD-IRF). In particular, the influence by other factors such as river stage on groundwater hydrographs can be explored by adding this as a stress within the IRF approach. It can be seen (e.g. Figure 10) that including this stress improves the simulation of groundwater hydrograph behaviour. This is particularly the case for the shallow boreholes which show a distinct influence from the river. Indeed proximity to rivers becomes an important factor in successfully deploying the combined AquiMOD-IRF approach.

4 | SUMMARY AND CONCLUSIONS

This paper has presented the application of both lumped parameter models (AquiMOD) and IRFs to help understand and characterize the groundwater flow processes of the St Bees and Penrith sandstones in the Eden valley, Cumbria. Using these techniques daily groundwater hydrographs from 2002 to 2012 have been analysed, four types of response identified in different regions of the aquifer: (1) St. Bees Sandstone; (2) in the Brockram; (3) in the silicified Penrith Sandstone; and (4) in the central part of the Penrith Sandstone heavily influenced by the interaction with rivers.

It is clear that AquiMOD, IRF and a combination of AquiMOD with IRF can be deployed to reproduce hydrograph responses in a range of hydrogeological settings. Importantly the choice of a variety of techniques demonstrates the influence of differing processes and hydrogeological settings. For example, where groundwater hydrographs are influenced by river stage variation then the AquiMOD-IRF approach produces. Further the relative importance of differences in water level time series behaviour between observation boreholes can be characterized. Nevertheless care must be taken in choosing the particular methodology to employ. For example, using double IRF which produce clear differences between the curves suggest difficulties in AquiMOD calibration.

This work has clearly shown that the use of the lumped parameter models and IRFs in the analysis of groundwater level time series can distinguish the influences of differing hydrogeological environments and the impacts these have on the groundwater flow processes. They can be used, as shown in this paper, in a staged approach to help develop reliable and comprehensive conceptual models of groundwater flow. This can then be used as a solid basis for the development of distributed models, particularly as the latter are resource expensive to build and to calibrate effectively. This approach of using simple models and techniques first identifies specific aspects of catchment functioning, for example influence of the river, that can be later tested in a distributed model. Further as demonstrated here, these techniques allow the identification of particular processes to be included in the distributed model, for example two timescales of response (fast and slow). For distributed models, the zonation of hydrograph response identified using these techniques can be used directly in providing an initial basis for the distribution of parameters. It has been demonstrated that these techniques can help in the definition of areas of significant heterogeneity, the influence of various lithological horizons and of surface water/groundwater interaction on the groundwater piezometric behaviour.

ACKNOWLEDGEMENTS

Hughes publishes with the permission of the Executive Director, British Geological Survey (UKRI). The work was funded by a grant (NE/I006591/1) under the NERC Changing Water Cycle programme. Dr Chris Jackson is gratefully acknowledged for his support in extending AquiMOD to include IRF. Dr Majdi Mansour is acknowledged for providing an internal BGS review. Two anonymous reviewers are thanked for their comments which helped improve the paper.

DATA AVAILABILITY STATEMENT

Data used in this paper are available from the Environment Agency and UK Met Office via the following APIs:

Groundwater levels: Shoothill API (riverlevelsapi.shoothill.com/help).

Rainfall: MetOffice API (www.metoffice.gov.uk/services/data/datapoint).

River stage: Environment Agency API (environment.data.gov.uk/hydrology/doc/reference#introduction).

MORECS Potential Evaporation was used under licence from the UK Met Office.

ORCID

Andrew G. Hughes https://orcid.org/0000-0001-9940-1813

REFERENCES

Abesser, C., Clarke, D., Hughes, A. G., & Robins, N. S. (2017). Modelling small groundwater systems: Experiences from the Braunton Burrows and Ainsdale coastal dune systems, UK. *Journal of Coastal Conservation*, *21*(5), 595–614. https://doi.org/10.1007/s11852-017-0525-5

Allen, D. J., Brewerton, L. J., Coleby, L. M., Gibbs, B. R., Lewis, M. A., MacDonald, A. M., Wagstaff, S. J., & Williams, A. T. (1997). The physical properties of major aquifers in England and Wales. British Geological Survey, 333pp. (WD/97/034) (Unpublished). http://nora.nerc.ac.uk/id/eprint/13137/

Anaya, R., & Wanakule, N. (1993). A lumped parameter model for the edwards aquifer. Texas Water Resources Institute. Available electronically from https://hdl.handle.net /1969.1/6172

Ascott, M. J., Marchant, B. P., Macdonald, D., McKenzie, A. A., & Bloomfield, J. P. (2017). Improved understanding of spatio-temporal controls on regional scale groundwater flooding using hydrograph analysis and impulse response functions. *Hydrological Processes*, *31* (25), 4586–4599. https://doi.org/10.1002/hyp.11380

Barrett, M., & Charbeneau, R. (1997). A parsimonious model for simulating flow in a karst aquifer. *Journal of Hydrology*, *196*, (1-4), 47–65.

Box, G. E., Jenkins, G. M., Reinsel, G. C., & Ljung, G. M. (2015). *Time series analysis: Forecasting and control*. (5th edn, 1), 712. Bridgewater, NJ: John Wiley.

Butcher, A., Lawrence, A., Jackson, C., Cullis, E., Cunningham, J., Hasan, K., & Ingram, J. J. (2006). Investigating rising nitrate concentrations in groundwater in the Permo-Triassic aquifer, Eden Valley, Cumbria, UK. *Geological Society*, *London*, *Special Publications*, *263*(1), 285–296.

Cowpertwait, P. S., & Metcalfe, A. V. (2009). Time series data. In *Introductory time series with R*. Springer.

Delbart, C., Valdés, D., Barbecot, F., Tognelli, A., & Couchoux, L. (2016). Spatial organization of the impulse response in a karst aquifer. *Journal of Hydrology*, *537*, 18–26. https://doi.org/10.1016/j.jhydrol.2016.03.029

Di Lazzaro, M., Zarlenga, A., & Volpi, E. (2015). Hydrological effects of within-catchment heterogeneity of drainage density. *Advances in Water Resources*, *76*, 157–167. https://doi.org/10.1016/j.advwatres.2014.12.011

Griffiths, J., Keller, V., Morris, D., & Young, A. (2008). Continuous estimation of river flows (CERF). Environment Agency Science Report SC030240, Bristol.

Hill, M. C., & Tiedeman, C. R. (2006). *Effective groundwater model calibration: With analysis of data*, *sensitivities*, *predictions*, *and uncertainty*, (1–480). John Wiley.

Hocking, M., & Kelly, B. F. J. (2016). Groundwater recharge and time lag measurement through Vertosols using impulse response functions. *Journal of Hydrology*, *535*, 22–35. https://doi.org/10.1016/j.jhydrol.2016.01.042

Hughes, D. A. (2004). Incorporating groundwater recharge and discharge functions into an existing monthly rainfall–runoff model. *Hydrological Sciences Journal*, *49*(2), 311. https://doi.org/10.1623/hysj.49.2.297.34834.

Hughes, R. A. (2003). Permian and Triassic rocks of the Appleby district (part of Sheet 30, England and Wales). http://nora.nerc.ac.uk/id/eprint/3674/1/RR02001.pdf

Hulme, P. J., Jackson, C. R., Atkins, J. K., Hughes, A. G., Mansour, M. M., Seymour, K. J., & Wilson, K. J. (2012). A rapid model for estimating the depletion in river flows due to groundwater abstraction. *Geological Society*, *London*, *Special Publications*, *364*(1), 289–302. https://doi.org/10.1144/sp364.18

Hutchins, M. G., Abesser, C., Prudhomme, C., Elliott, J. A., Bloomfield, J. P., Mansour, M. M., & Hitt, O. E. (2018). Combined impacts of future land-use and climate stressors on water resources and quality in groundwater and surface waterbodies of the upper Thames river basin, UK. *Science of the Total Environment*, *631–632*, 962–986. https://doi.org/10.1016/j.scitotenv.2018.03.052

Jackson, C. R., Hughes, A. G., Dochartaigh, B. E. O., Robins, N. S., & Peach, D. W. (2005). Numerical testing of conceptual models of groundwater flow: A case study using the Dumfries Basin aquifer. *Scottish Journal of Geology*, *41*, 51–60.

Jackson, C. R., Meister, R., & Prudhomme, C. (2011). Modelling the effects of climate change and its uncertainty on UK Chalk groundwater resources from an ensemble of global climate model projections. *Journal of Hydrology*, *399*(1–2), 12–28. https://doi.org/10.1016/j.jhydrol.2010.12.028

Lafare, A. E. A., Hughes, A. G., & Peach, D. W. (2014). *Eden Valley observation boreholes: Hydrogeological framework and groundwater level time series analysis*. see http://nora.nerc.ac.uk/id/eprint/508772/

Lafare, A. E. A., Peach, D. W., & Hughes, A. G. (2016). Use of seasonal trend decomposition to understand groundwater behaviour in the Permo-Triassic Sandstone aquifer, Eden Valley, UK. *Hydrogeology Journal*, *24*(1), 141–158. https://doi.org/10.1007/s10040-015-1309-3

Leedal, D., Weerts, A. H., Smith, P. J., & Beven, K. J. (2013). Application of data-based mechanistic modelling for flood forecasting at multiple locations in the Eden catchment in the National Flood Forecasting System (England and Wales). *Hydrology and Earth System Sciences*, *17* (1), 177–185. https://doi.org/10.5194/hess-17-177-2013

Long, A. J. (2015). RRAWFLOW: Rainfall-response aquifer and watershed flow model (v1.15). *Geoscientific Model Development*, *8*(3), 865–880. https://doi.org/10.5194/gmd-8-865-2015

Long, A. J., & Mahler, B. J. (2013). Prediction, time variance, and classification of hydraulic response to recharge in two karst aquifers. *Hydrology* *and Earth System Sciences*, *17*(1), 281–294. https://doi.org/10.5194/hess-17-281-2013

Mackay, J. D., Jackson, C. R., & Wang, L. (2014a). *AquiMod user manual (v1.0)*. see http://nora.nerc.ac.uk/id/eprint/507668/

Mackay, J. D., Jackson, C. R., & Wang, L. (2014b). A lumped conceptual model to simulate groundwater level time-series. *Environmental Modelling & Software*, *61*, 229–245. https://doi.org/10.1016/j.envsoft.2014.06.003

Mackay, J. D., Jackson, C. R., Brookshaw, A., Scaife, A. A., Cook, J., & Ward, R. S. (2015). Seasonal forecasting of groundwater levels in principal aquifers of the United Kingdom. *Journal of Hydrology*, *530*, 815–828. https://doi.org/10.1016/j.jhydrol.2015.10.018.

Mangin, A. (1984). Pour une meilleure connaissance des systèmes hydrologiques à partir des analyses corrélatoire et spectrale. *Journal of Hydrology*, *67*(1), 25–43. https://doi.org/10.1016/0022-1694(84)90230-0

Mayes, W. M., Walsh, C. L., Bathurst, J. C., Kilsby, C. G., Quinn, P. F., Wilkinson, M. E., Daugherty, A. J., & O'Connell, P. E. (2006). Monitoring a flood event in a densely instrumented catchment, the Upper Eden, Cumbria, UK. *Water and Environment Journal*, *20*(4), 217–226. https://doi.org/10.1111/j.1747-6593.2005.00006.x

Millward, D. (2004). Geology of the Appleby district: A brief explanation of the geological map Sheet 30 Appleby. https://webapps.bgs.ac.uk/data/publications/pubs.cfc?method=viewRecord&publnId=19868134

Oudin, L., Kay, A., Andréassian, V., & Perrin, C. (2010). Are seemingly physically similar catchments truly hydrologically similar? *Water Resources Research*, *46*(11), W11558. https://doi.org/10.1029/2009wr008887

Rogger, M., Agnoletti, M., Alaoui, A., Bathurst, J. C., Bodner, G., Borga, M., Chaplot, V., Gallart, F., Glatzel, G., Hall, J., Holden, J., Holko, L., Horn, R., Kiss, A., Kohnová, S., Leitinger, G., Lennartz, B., Parajka, J., Perdigão, R., … Bloschl, G. (2017). Land use change impacts on floods at the catchment scale: Challenges and opportunities for future research. *Water Resources Research*, *53*(7), 5209–5219. https://doi.org/10.1002/2017WR020723

Rozos, E., Efstratiadis, A., Nalbantis, I., & Koutsoyiannis, D. (2004). Calibration of a semi-distributed model for conjunctive simulation of surface and groundwater flows/Calage d'un modèle semi-distribué pour la simulation conjointe d'écoulements superficiels et souterrains. *Hydrological Sciences Journal*, *49*(5), 842. https://doi.org/10.1623/hysj.49.5.819.55130

Russo, T. A., & Lall, U. (2017). Depletion and response of deep groundwater to climate-induced pumping variability. *Nature Geoscience*, *10*(2), 105–108. https://doi.org/10.1038/ngeo2883

Scanlon, B. R., Mace, R. E., Barrett, M. E., & Smith, B. (2003). Can we simulate regional groundwater flow in a karst system using equivalent porous media models? Case study, Barton Springs Edwards aquifer, USA. *Journal of Hydrology*, *276*(1–4), 137–158. https://doi.org/10.1016/s0022-1694(03)00064-7

Schilling, O. S., Cook, P. G., & Brunner, P. (2019). Beyond classical observations in hydrogeology: The advantages of including exchange flux, temperature, tracer concentration, residence time, and soil moisture observations in groundwater model calibration. *Reviews of Geophysics*, *57*(1), 146–182. https://doi.org/10.1029/2018RG000619

Stone, P., Millward, D., Young, B., Merritt, J. W., Clarke, S. M., McCormac, M., & Lawrence, D. J. D. (2010). British regional geology: Northern England. Fifth edition. Keyworth, Nottingham: British Geological Survey. https://webapps.bgs.ac.uk/data/publications/pubs.cfc?method=viewRecord&publnId=19868134

van der Spek, J. E., & Bakker, M. (2017). The influence of the length of the calibration period and observation frequency on predictive uncertainty in time series modeling of groundwater dynamics. *Water Resources Research*, *53*(3), 2294–2311. https://doi.org/10.1002/2016wr019704

von Asmuth, J. R., Bierkens, M. F. P., & Maas, K. (2002). Transfer function-noise modeling in continuous time using predefined impulse response functions. *Water Resources Research*, *38*(12), 23-1–23-12. https://doi.org/10.1029/2001wr001136

von Asmuth, J. R., Maas, K., Bakker, M., & Petersen, J. (2008). Modeling time series of ground water head fluctuations subjected to multiple stresses. *Ground Water*, *46*(1), 30–40. https://doi.org/10.1111/j.1745-6584.2007.00382.x

Wang, L., & Burke, S. P. (2017). A catchment-scale method to simulating the impact of historical nitrate loading from agricultural land on the nitrate-concentration trends in the sandstone aquifers in the Eden Valley, UK. *Science of the Total Environment*, *579*, 133–148. https://doi.org/10.1016/j.scitotenv.2016.10.235

Waugh, B. (1970). Petrology, provenance and silica diagenesis of the Penrith sandstone (lower Permian) of Northwest England. *Journal of Sedimentary Research*, *40*, 1226–1240.

How to cite this article: Lafare AEA, Peach DW, Hughes AG. Use of point scale models to improve conceptual understanding in complex aquifers: An example from a sandstone aquifer in the Eden valley, Cumbria, UK. *Hydrological Processes*. 2021;35:e14143. https://doi.org/10.1002/hyp.14143

APPENDIX A.

Implementing the impulse response function with stresses within AquiMOD (AquiMOD-IRF)

According to Von Asmuth et al. (2008), in continuous time, the contribution from each stress to the groundwater level fluctuations time series can be represented by the following equation:

$$h_i(t) = \int_{-\infty}^{t} R_i(\tau)\theta_i(t-\tau)d\tau, \tag{A1}$$

where h_i[L] is the predicted head at time *t* attributable to stress *i*. R_i is the value of stress *i* at time *t*, and θ_i is the IRF of stress *i*. The output groundwater head fluctuations time series is then obtained by summing the separate effects of all stresses. For the case where a number of *N* stresses influence the head, the equation for a continuous groundwater level time series model can be written as:

$$h(t) = \sum_{i=1}^{N} h_i(t) + d + n(t), \tag{A2}$$

where *h* is the observed head at time *t*, *d* is the local drainage level relative to some reference level [L], and *n* is the residual series [L].

Von Asmuth et al. (2008) distinguish a number of stresses that potentially influence the groundwater level fluctuations, including precipitation (*p*), evaporation (*e*), groundwater withdrawal (or injection) (*w*), surface water level or river stage, barometric pressure and (hydrological) interventions. Currently, only the stresses: precipitation, evaporation and withdrawal, along with river stage have been implemented in the AquiMOD software. The effect of the evaporation *e* on the head *h* is considered to be essentially the same as that of precipitation *p*, but it is negative and is modelled as follows:

$$h_e(t) = \int_{-\infty}^{t} -e(\tau) f \theta_p(t-\tau) d\tau, \tag{A3}$$

where θ_p is the response of the system to precipitation and *f* is a reduction factor of *e* as compared to the reference evaporation series. The response of an impulse of precipitation is simulated using a Pearson type III distribution function (PIII):

$$\theta_p(t) = A \frac{b^n t^{n-1} \exp(-bt)}{\Gamma(n)}, \tag{A4}$$

where *A*, *b*, and *n* are parameters that define the shape of θ_p. Although the PIII function is very flexible, it proves to be less effective for non-distributed types of stress. For surface water level fluctuations response functions based on analytical solutions of simple hydrogeological conceptualisations are proposed. It is assumed that the functions chosen capture the essential behaviour of the stress type regardless the exact hydrogeological setting. For this kind of stress, the polder function of Bruggeman (Von Asmuth et al., 2008) is used. This function represents a sudden unit increase of the water level at the boundary of a one-dimensional semi-confined aquifer of semi-infinite extent. The derivative gives the IRF θ_s, the response to a very short rise and fall of the surface water level:

$$\theta_s(t) = \frac{-1}{\sqrt{\frac{4\pi k D t^3}{x^2 S}}} \exp\left(\frac{-x^2 S}{4kDt} - \frac{t}{cS}\right), \tag{A5}$$

where *x* denotes the distance between the surface water feature and the observation well. In order to make the IRF usable for different hydrogeological settings, the equation is converted to the following parametric IRF:

$$\theta_s(t) = \frac{-\gamma}{\sqrt{\pi \frac{\beta^2}{\alpha^2} t^3}} \exp\left(\frac{-\alpha^2}{\beta^2 t} - \beta^2 t\right), \tag{A6}$$

where α, β, and γ are parameters that no longer have a direct physical meaning (Von Asmuth et al., 2008).